Appl. Phys. B 70, 15–21 (2000) / Digital Object Identifier (DOI) 10.1007/s003409900103

Applied Physics B
Lasers
and Optics

A two-stage up-convertor made of $AgGaSe_2$ and β-BBO crystals

H.-w. Wang, M.-h. Lu

Institute of Electro-optical Engineering, National Chiao-Tung University, 1001 Ta Hsueh Road, Hsinchu 300, Taiwan, Republic of China
(Fax: +886-03/5716-631, E-mail: u8224814@cc.nctu.edu.tw)

Received: 4 January 1999/Revised version: 19 May 1999/Published online: 25 August 1999

Abstract. A two-stage infrared up-convertor made of $AgGaSe_2$ and β-BBO crystals has been built up, that can up-convert the mid-infrared radiation of 11–16 μm into the 0.8-μm range where the sensitive photomultiplier can be used. This up-convertor is pumped with a near-infrared radiation of 1.7–1.8 μm wavelength range generated by a β-BBO optical parametric oscillator.

In this experiment, we also measured the o-ray refractive index of $AgGaSe_2$ in the 11–16 μm mid-infrared range and extended the fitting range of the Sellmeier equation to the 16-μm wavelength range.

PACS: 42.65; 42.70

Silver thiogallate crystal ($AgGaS_2$) and silver selenogallate crystal ($AgGaSe_2$) with chalcopyrite structure (point group $\bar{4}2m$) are very useful nonlinear optical elements used in the near-infrared (NIR) to mid-infrared (MIR) range [1, 2]. Since the $AgGaS_2$ crystal has a cut-off wavelength of transmission at 13 μm, in the application of the parametric conversion for the wavelength longer than 13 μm we must choose the $AgGaSe_2$ crystal. It has an optical transmission over a range from 0.71 to 18 μm. Recently, there has been an advance in $AgGaSe_2$ crystal fabrication, so the high conversion efficiency, and large dimension for this crystal has become available [3]. An energy conversion efficiency of 21% for the second-harmonic generation of a CO_2 laser [4] and the damage threshold 16 MW/cm^2 for a laser pulse [5] have been reported. Many papers have been published concerning applications of this crystal on the double frequency of CW [2] and pulsed [6] CO_2 lasers, wavelength-tunable optical parametric oscillators (OPO) [7], and IR up-conversion [8].

The IR up-conversion is a useful technique for infrared detection because it has fast-response and highly sensitive characteristics at room temperature. We had used β-BBO crystal and $AgGaS_2$ crystal in IR up-conversion for the measurement of IR spectroscopy in the 1–3 μm range [9] and 3–9 μm range [10], respectively. Recently we built up a two-stage up-convertor which consists of $AgGaSe_2$ and β-BBO crystals. In the first stage $AgGaSe_2$, the MIR wave of the 11–16 μm range was mixed with the pumping wave from an OPO in type I (oo→e), and up-converted into the 1.5-μm range. In the second stage β-BBO, the up-converted wave from the first stage was mixed with the pumping wave and up-converted again into the 0.8-μm range. The final up-converted radiation could be detected by a sensitive photomultiplier tube (PMT). A β-BBO optical parametric oscillator (OPO) which generates a NIR emission of 1.7–1.8 μm was used as pumping source for this up-convertor.

This two-stage up-convertor made of $AgGaSe_2$/β-BBO has a much wider up-conversion range, and a simpler structure than those made of the $AgGaS_2/LiIO_3$ [11, 12], $Ag_3AsS_3/LiIO_3$, $ZnGeP_2/LiIO_3$, and $HgGa_2S_4/LiIO_3$ [12].

In the $AgGaSe_2$ stage, the OPO radiation (o-ray) and the generated up-converted wave (e-ray) have vertical and horizontal polarization, respectively. When these two waves reach the second stage β-BBO, the large birefringence of $AgGaSe_2$ causes a big walk-off angle for the up-converted beam (e-ray) generated in this crystal. When both beams reach the second stage, the separation between them could be so large that they can not spatially overlap well under phase-matching condition. This could be the main reason that the type-II (oe→e) process not be observed in the second stage in this work. In order to solve this problem, we used a scheme called polarization bypass. It will be discussed later.

In this up-conversion experiment, we found that the measured phase-matching angles for the wavelength longer than 13.5 μm were obviously different from those calculated with the Sellmeier equations given by Kidal et al. [13], Bhar [14], Roberts [15], and Harasaki et al. [16]. With the measured external incident angle under phase-matching condition for $AgGaSe_2$, we calculated the $AgGaSe_2$ refractive indices of o-ray in the 11–16 μm range. Based on our data and Boyd et al.'s data [17], we propose an improved Sellmeier equation of the o-ray refractive index for $AgGaSe_2$ in the 0.85–16 μm range.

1 Experiment

The setup of the two-stage up-convertor is schematically shown in Fig. 1. The measured MIR radiations were generated by the potassium vapor excited on the 4S-8S or 4S-6D two-photon resonance with a pulsed DCM dye laser, pumped by a frequency-doubled Nd:YAG pulsed laser. These IR amplified spontaneous emissions (ASE) are from the atomic transitions of $8S_{1/2}$–$7P_{3/2,1/2}$, $7P_{3/2,1/2}$–$7S_{1/2}$, $6D_{5/2}$–$7P_{3/2}$, $6D_{3/2}$–$7P_{3/2,1/2}$, and $7P_{3/2,1/2}$–$5D_{3/2,5/2}$, as shown in Fig. 2. The potassium vapor which generated the IR emissions was enclosed in a heat pipe [18] and heated to a temperature about 370 °C with 30-cm heated zone. Argon gas of 2.5 Torr was used as a buffer gas in the heat pipe. The entrance window of the heat pipe was quartz and the exit window was ZnSe. Typical operating parameters for the DCM dye laser tuned to a wavelength of 629.6 nm or 631.0 nm were 6 ns pulse duration, 10 mJ pulse energy, 0.2 cm^{-1} linewidth, and 10 Hz repetition rate. The dye laser beam was focused by a lens of 100 cm focal length into a spot with a diameter of 0.25 mm at the center of the heat pipe.

An OPO is composed of a resonant cavity made of two parallel mirrors where a β-BBO crystal (Fujian Institute of Research on the Structure of Matter) locates in between. The β-BBO crystal has dimensions of $10 \times 10 \times 10$ mm with a cut angle of $\theta = 30°$ and $\phi = 0°$. The OPO pumped by a triple-frequency Nd:YAG pulsed laser which has 20 ns pulse duration, 43 mJ pulse energy, 0.25 cm^{-1} linewidth, and 10 Hz repetition rate. The two output beams of OPO, one of which is visible and the other is NIR, are wavelength tunable with angle tuning of the crystal in the resonant cavity. The NIR beam of 1.7–1.8 μm with 1 mm spot size, 1.75 mrad divergence angle, and 0.4 mJ pulse energy, is used as the pumping source of up-conversion. In order to compensate the large walk-off effect in $AgGaSe_2$ as we mentioned before, we used a circularly polarized pumping wave instead of a linearly polarized wave. A Soleil-Babinet compensator (Mells Griot Co.) was put in the NIR beam, which converted the polarization of the OPO beam from linear into circular. The NIR pumping beam and MIR radiations were collinearly incident upon the two-stage up-convertor with a 45° dichroic mirror. In order to ensure the temporal overlap of the OPO radiation and the MIR radiation in the crystals, a pulse delay generator was used for the exact timing of the two YAG lasers, as shown in Fig. 1.

When the pumping wave enters the $AgGaSe_2$, as shown in Fig. 3, it will be divided into two beams. One has linear vertical polarization used as pumping wave (o-ray) for the first stage and the other has linear horizontal polarization. The latter passes through the $AgGaSe_2$ stage and is used as pumping wave for the second stage. This polarization bypass is similar to that used in third-harmonic generation (THG) with two identical KDP crystals [19]. Since the up-converted beam and the horizontally linear polarized OPO beam are both the e-rays in the $AgGaSe_2$, both of them suffer from the same walk-off effect.

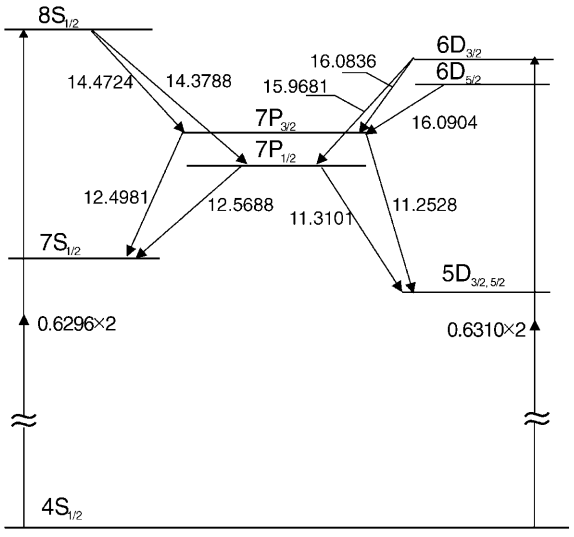

Fig. 2. Partial energy level diagram of potassium showing the related processes in the experiment. All the wavelengths are in μm

Since all the MIR emissions are stimulated by the dye laser, we can consider these IR emissions and the laser beam as collinear. It means that if we make the OPO and dye laser beams collinear, the OPO beam and the IR emissions can be considered to be collinear too. After the spatial overlap of the MIR emissions and the OPO beam had been made, we put a Ge plate behind the heat pipe to blockade the strong DCM dye laser 629.6 nm or 631.0 nm and to transmit the MIR emissions.

The two crystals used in this two-stage up-convertor are: (i) $AgGaSe_2$ crystal (EKSMA Co.) which has dimensions of $10 \times 10 \times 10$ mm with a cut angle of $\theta = 45.2° \pm 0.1°$ and $\phi = 45°$, and (ii) β-BBO crystal (Fujian Institute of Research on the Structure of Matter) which has $9.5 \times 10 \times 6.9$ mm with a cut angle of $\theta = 23.1° \pm 0.1°$ and $\phi = 0°$.

The spacing between the $AgGaSe_2$ and β-BBO stages is 5 mm, and the optical axis planes of the two stages are perpendicular to each other. Both the crystals in this two-stage

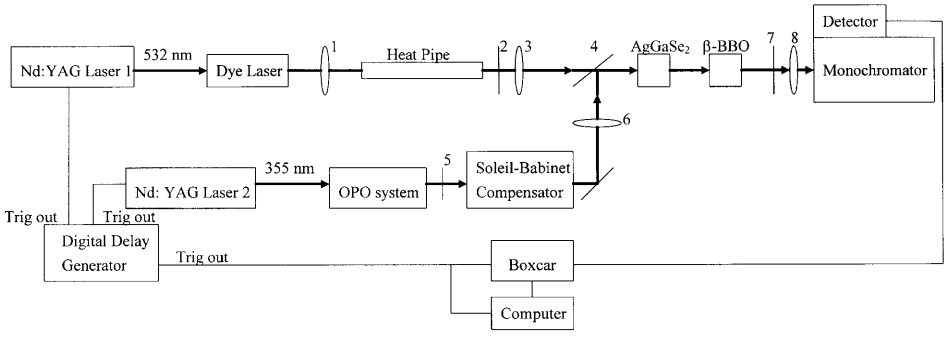

Fig. 1. The setup diagram of two-stage up-convertor system: 1) BK7 lens; 2) Ge mirror; 3) ZnSe lens; 4) 45° dichroic mirror; 5) Colored glass filter; 6) BK7 lens; 7) IR polarizer or bandpass filter; 8) BK7 lens

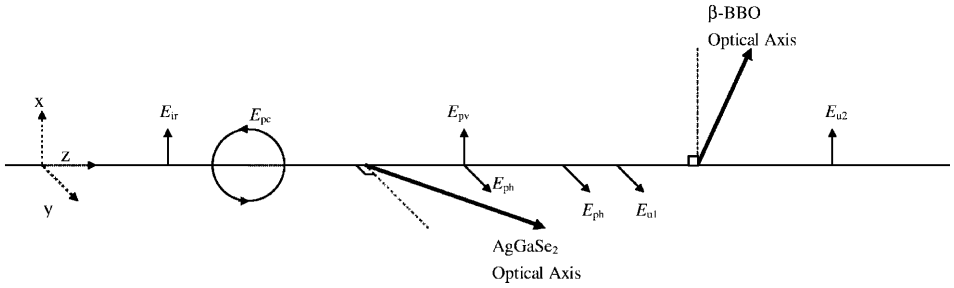

Fig. 3. The polarization diagram of the various beams. E_{ir} represents the polarization of the measured MIR radiation. E_{pc}, E_{pv}, and E_{ph} represent the circular, vertical, and horizontal polarizations of OPO wave, respectively. E_{u1} and E_{u2} represent the polarizations of up-converted signals from the first stage and two stages, respectively

up-convertor were operated in type I (oo→e). The OPO beam and the measured MIR radiations were focused on the two-stage up-convertor by a BK7 lens of focal length 250 mm and a ZnSe lens of focal length 170 mm, respectively. The spot size of the OPO beam is 1 mm on the $AgGaSe_2$ surface and is 1.35 mm on the β-BBO surface. The OPO wave intensities of vertical polarization and horizontal polarization are measured to be 1.2×10^6 W/cm^2 at the $AgGaSe_2$ and 6.3×10^5 W/cm^2 at the β-BBO, respectively. The spot size of the MIR radiation can be considered as the same as that of the dye laser, which is about 0.9 mm on the $AgGaSe_2$. The divergence angle of the MIR beam is 3.5 mrad.

We took the Soleil-Babinet compensator off and put an IR polarizer behind the up-convertor to blockade the strong OPO beam when the up-converted signal from the first stage was measured with a Ge detector (Hamamatsu B1919-01). Then we removed IR polarizer, put a band-pass filter behind the up-convertor, and detected the final two-stage up-converted signal with PMT (Hamamatsu R636). In all the measurements a 1-m monochromator (Spex 1704) with a grating of 600 l/mm was used.

2 Results and discussion

The propagations of various beams in the two-stage up-convertor are shown in Fig. 4. In the $AgGaSe_2$ stage, the vertically polarized component K_{pv} of the OPO beam and MIR beam K_{ir} are mixed in type I (oo→e). In this process the walk-off effect causes an angular deviation of the up-converted beam from its wave vector. As mentioned before, the influence of this walk-off effect on the up-conversion of the second stage can be compensated by the fact that the horizontally polarized OPO beam used as the pumping wave in the second stage suffers from the same walk-off effect. For instance, if the 16.05-μm MIR emisson and the 1.75-μm OPO beam are collinearly incident upon the $AgGaSe_2$ stage, under phase-matching condition the external incident angle is 6.90°. In this case, according to our calculation, between these two stages the angle δ and the separation l between the up-converted beam K_{u1} and the horizontally polarized OPO beam K_{ph} are $\approx 5 \times 10^{-5}$ degree and ≈ 6 μm, respectively, see Fig. 4. It means that the both beams are almost collinear when they are incident upon the β-BBO. However, the separation l' between the up-converted beam K_{u1} and the vertically polarized OPO beam K_{pv} are ≈ 112 μm, which is so large that the K_{u1} and K_{pv} can not spatially overlap well in β-BBO under phase-matching condition. Besides, calculating the conversion efficiencies, we find that the conversion efficiency of power for type I (oo→e) is 30 times as large as that of type II (oe→e). Therefore, in this β-BBO stage the wave-mixing of type I (oo→e) is much more effective.

The MIR emissions in the 11–16 μm range from the excited potassium atoms were up-converted with this $AgGaSe_2$/β-BBO two-stage up-convertor into the 0.8-μm range. The measured signals from the first and the second stage are shown in Figs. 5 and 6. We find that the signals from the two-stage up-convertor have much higher signal-to-noise ratio than those from the first stage. The two-stage up-conversion detection system appears more sensitive than the one-stage up-conversion detection system. With the same entrance and exit slit widths of monochromator, the ratio of the signal from the two-stage up-convertor to that from one-stage is measured to be ≈ 4. This ratio can be evaluated by

$$r = \frac{\eta_{12}^{p} R_2}{\eta_1^{p} R_1} = \frac{\eta_2^{p} R_2}{R_1} , \tag{1}$$

and

$$\eta_{12}^{p} = \eta_1^{p} \eta_2^{p} ,$$

where R_1 and R_2 are the responsivities of the Ge detection system and the PMT detection system, respectively. η_1^{p} and η_2^{p} are the power efficiencies of $AgGaSe_2$ and β-BBO crystals, respectively. In this experiment, the R_1 and R_2 were measured to be 4.8×10^{-5} V/W at 1.57 μm and 2.7×10^{-2} V/W at 825 nm, respectively. Here all the effects of the detection system on the responsivity have been included. By using the equation of conversion efficiency in the plane-wave approximation [20], the η_2^{p}, relating to $\omega(1.57\,\mu\text{m}) + \omega_p(1.74\,\mu\text{m}) \rightarrow \omega(0.8253\,\mu\text{m})$ process in β-BBO, is caculated to be 6.8×10^{-3} at the pumping laser intensity 6.3×10^5 W/cm^2. From (1) we obtain the ratio r is 3.82, which agrees well with our measured ratio 4.

According to the noise theory of infrared detection by optical mixing [21], we estimated the noise-equivalent power (NEP) of two-stage up-conversion system. In this case the shot noise in dark current is considered to be the dominant noise source in PMT, and the quantum efficiency for two-stage up-convertor can be expressed as

$$\eta = \eta_1^{q} \eta_2^{q} , \tag{2}$$

where η_1^{q} and η_2^{q} are the quantum efficiencies of $AgGaSe_2$ and β-BBO, respectively. For the wave-mixing process, $\omega(16.06\,\mu\text{m}) + \omega_p(1.74\,\mu\text{m}) \rightarrow \omega(1.57\,\mu\text{m})$ in $AgGaSe_2$, we caculated $\eta_1^{q} = 4.7 \times 10^{-2}$ at the pumping laser intensity 1.2×10^6 W/cm^2. For the process, $\omega(1.57\,\mu\text{m}) + \omega_p(1.74\,\mu\text{m}) \rightarrow \omega(0.8253\,\mu\text{m})$ in β-BBO, we caculated $\eta_2^{q} =$

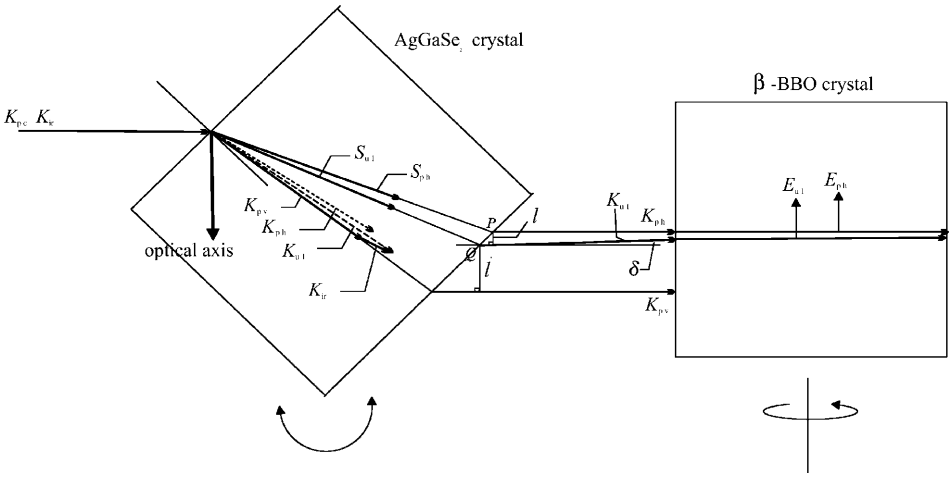

Fig. 4. The beam propagation digram in the $AgGaSe_2$/β-BBO two-stage up-convertor. Here the K, S, and E represent wave vector, Poynting vector and polarization, respectively. The subscripts pc, pv, and ph represent the circularly, vertically, and horizontally polarized OPO beams, respectively. The subscripts ir and u1 represent the MIR radiation and the up-converted beam generated in the first stage, respectively. δ is the angle between the K_{u1} and K_{ph}. l is the distance from the point P to K_{u1}, and l' is the distance from the point Q to K_{pv}

3.6×10^{-3} at the pumping laser intensity $6.3 \times 10^5\,W/cm^2$. The NEP of PMT (Hamamatsu R636) is taken to be $3.7 \times 10^{-13}\,W/Hz^{1/2}$. Thus we obtain the threshold of sensitivity for the two-stage up-convertor in the 16-μm region is $\approx 6.3 \times 10^{-11}\,W/Hz^{1/2}$.

We also noticed that some fine structures of MIR spectral lines can not be resolved. In this experiment the resolution of wavelength is mainly limited by the linewidth (≈ 2 nm) of OPO wave. Those fine structures could be resolved if the linewidth of OPO is less than 0.12 nm. The calculated and measured wavelengths of the both up-converted signals, and the related external incident angles on the both crystals are listed in Table 1, in which the errors in the measurements of the external incident angles for $AgGaSe_2$ and β-BBO are $\pm 0.5°$ and $\pm 0.05°$, respectively.

This two-stage up-convertor can be easily used to measure the MIR radiations from 11 μm to 16 μm. Besides, since the wavelengths of the resultant signals in the two-stage up-convertor are far from the wavelength of pumping wave, it becomes easier to filter against the strong pumping wave.

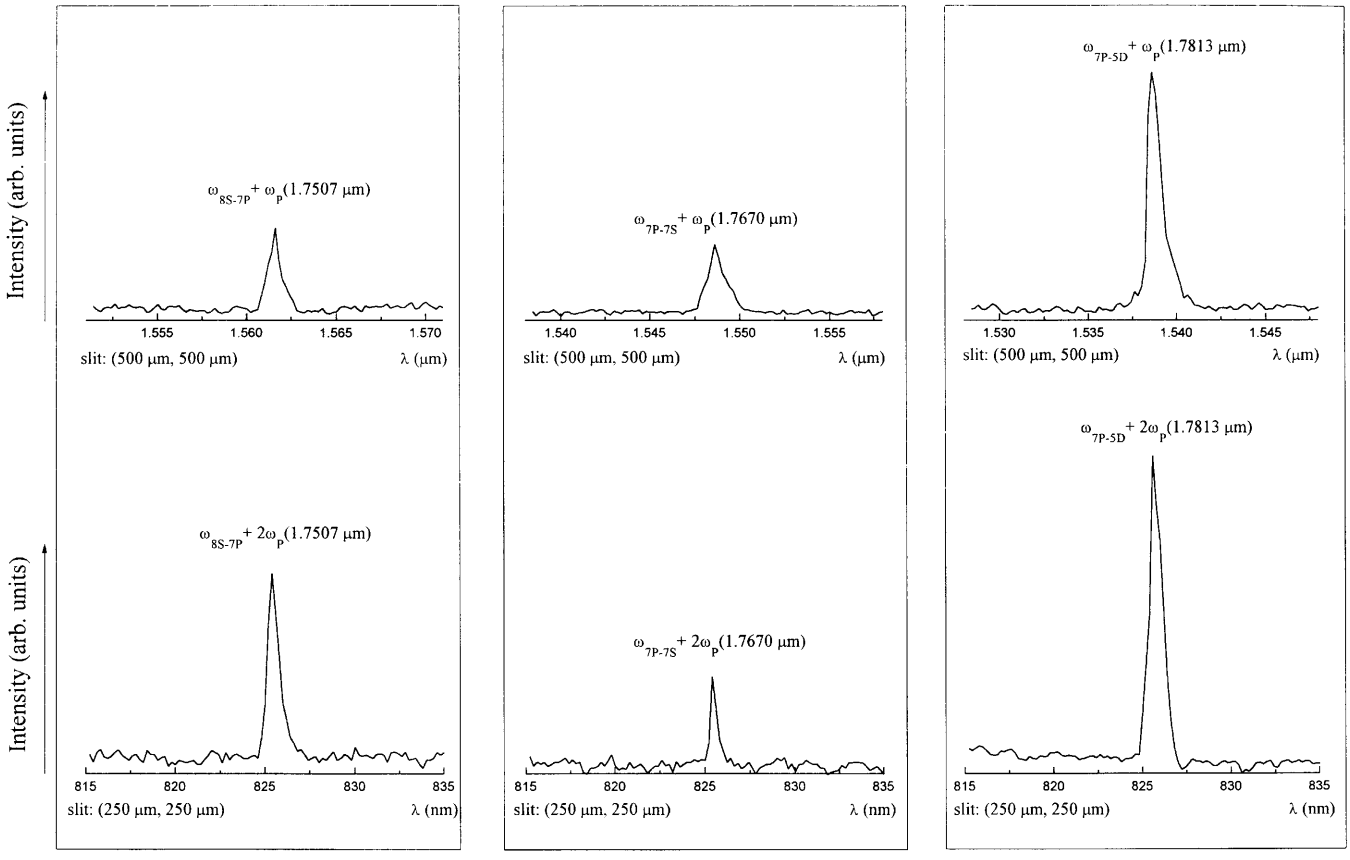

Fig. 5. The spectra measured with one-stage and two-stage up-convertors as the potassium was excited on the 4S-8S two-photon resonance. *Upper part* is the signals of the first stage and the *lower part* is the signals of the two-stage up-convertor. When we measured the signals from the first stage, the Soleil-Babinet compensator was removed

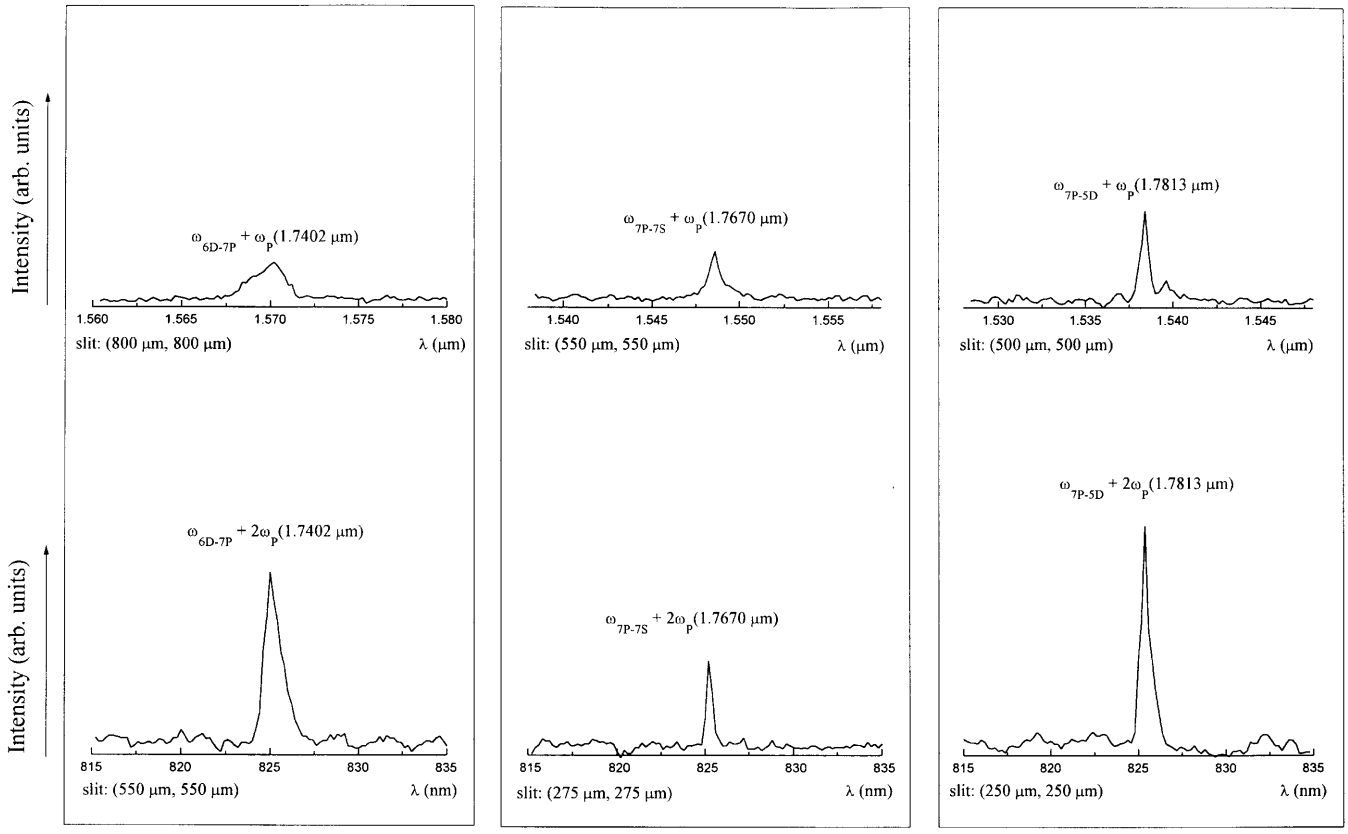

Fig. 6. The spectra measured with one-stage and two-stage up-convertors as the potassium was excited on the 4S-6D two-photon resonance. *Upper part* is for the signals of the $AgGaSe_2$ stage and the *lower part* is for the signals of the two-stage up-convertor. When we measured the signals from the $AgGaSe_2$ stage, the Soleil-Babinet compensator was removed

In a type-I phase-matched configuration of $AgGaSe_2$, as shown in Fig. 4, we have the following equations:

$$K_{u1}^2 = K_{pv}^2 + K_{ir}^2 - 2K_{pv}K_{ir}\cos[\pi - \theta_1 + \theta_2]\,, \tag{3}$$

$$K_{ir}^2 = K_{u1}^2 + K_{pv}^2 - 2K_{pv}K_{u1}\cos q\,, \tag{4}$$

$$K_{u1} = \frac{2\pi n_{u1}^{o}(\lambda) n_{u1}^{e}(\lambda)}{\lambda_{u1}\sqrt{[n_{u1}^{o}(\lambda)\sin\theta_m]^2 + [n_{u1}^{e}(\lambda)\cos\theta_m]^2}}\,, \tag{5}$$

where $K_{ir} = 2\pi n_{ir}^{o}(\lambda)/\lambda_{ir}$, $K_{pv} = 2\pi n_{pv}^{o}(\lambda)/\lambda_{pv}$, $\theta_1 = \sin^{-1} \times[\sin\theta_E/n_{ir}^{o}(\lambda)]$, and $\theta_2 = \sin^{-1}[\sin\theta_E/n_{pv}^{o}(\lambda)]$. K, λ, and n represent wave vector, wavelength in free space, and refractive index, respectively. Superscripts o and e denote ordinary and extraordinary waves, respectively. Subscripts ir, pv, u1 denote the MIR radiation, vertically polarized OPO beam, and the up-converted beam generated in the $AgGaSe_2$, respectively. q is the angle between K_{pv} and K_{u1}. θ_E is the external angle under phase-matching condition. The phase-matching angle $\theta_m = \theta_2 + q + \theta_C$, in which θ_C is the cut angle of $AgGaSe_2$. With the measurements of $\lambda_{pv}(=\lambda_p)$, θ_E, and λ_{u1}, as listed in Table 1, the refractive indices of o-ray n_o for $AgGaSe_2$ in the 11–16 μm range can be calculated with the (3)–(5) and are listed in Table 2. The errors of the refractive-index data listed in Table 2 are caused by the following three facts: (i) the resolution of the monochromator, (ii) the uncertainty in cut angle, and (iii) the uncertainty in the measurement of the external incident angle under phase-matching condition.

Based on our refractive-index data in the 11–16 μm range listed in Table 2 and Boyd et al.'s data in the 0.85–13.5 μm range [17], we have the following improved Sellmeier equation

$$n_o^2 = A + \frac{B}{\lambda^2 + C} + \frac{D}{\lambda^2 + E} + F\lambda^2 + G\lambda^4 + H\lambda^6\,. \tag{6}$$

Here,

$$A = 6.85472\,; \quad B = 0.421498\,; \quad C = -0.168867\,;$$
$$D = -0.000872412\,; \quad E = -2.78693\,; \quad F = -0.001416\,;$$
$$G = 1.78628 \times 10^{-6}\,; \quad H = -5.78598 \times 10^{-9}\,,$$

where the n_o is the o-ray refractive index and λ is the wavelength in μm. The n_o^2 curve is illustrated in Fig. 7. The standard deviation of n_o given by (6) from the source data is 3.5×10^{-4}. For comparison we calculated the o-ray refractive indices with the Sellmeier equations given by this work and Harasaki et al.'s work [16]. The results are listed in Table 3. The uncertainty of the refractive-index data is ($\pm 1 \times 10^{-3}$). Actually, our data agree well with Harasaki et al.'s data for the wavelength shorter than 13.5 μm. However, for the wavelength longer than 13.5 μm the difference between our data and Harasaki et al.'s data increases as the wavelength increases. According to the Harasaki et al.'s equation, the calculated external incident angle under phase matching is 1.5° less than our measured value at 16 μm.

Table 1. The wavelengths of pumping waves, MIR emissions expected to be observed, calculated and measured up-converted signals, and external incident angles of crystals in the $AgGaSe_2$/β-BBO two-stage up-convertor under phase-matching condition of type I

pumping wavelength in the up-conversion process λ_p (μm)	IR wavelength predicted from the related transition λ_{ir} (μm)	up-converted signal wavelength from the first stage $AgGaSe_2$ λ_{u1} (μm) calculated	measured	up-converted signal wavelength from the second stage β-BBO λ_{u2} (nm) calculated	measured	external incident angle (degree) $AgGaSe_2$ (θ_E)	β-BBO
$1.7402 \pm 1 \times 10^{-4}$	15.9681 $6D_{3/2}$–$7P_{1/2}$	1.5691	$1.5702 \pm 6 \times 10^{-4}$	825.1	825.0 ± 0.5	7.1 ± 0.5	4.98 ± 0.05
	16.0836 $6D_{3/2}$–$7P_{3/2}$	1.5702		825.4			
	16.0904 $6D_{5/2}$–$7P_{3/2}$	1.5703		825.4			
$1.7507 \pm 1 \times 10^{-4}$	14.3788 $8S_{1/2}$–$7P_{1/2}$	1.5606	$1.5616 \pm 4 \times 10^{-4}$	825.1	825.4 ± 0.2	8.2 ± 0.5	4.40 ± 0.05
	14.4724 $8S_{1/2}$–$7P_{3/2}$	1.5617		825.4			
$1.7670 \pm 1 \times 10^{-4}$	12.4981 $7P_{3/2}$–$7S_{1/2}$	1.5481	$1.5486 \pm 4 \times 10^{-4}$	825.1	825.2 ± 0.2	11.8 ± 0.5	4.43 ± 0.05
	12.5688 $7P_{1/2}$–$7S_{1/2}$	1.5492		825.4			
$1.7813 \pm 1 \times 10^{-4}$	11.2528 $7P_{3/2}$–$5D_{3/2,5/2}$	1.5378	$1.5386 \pm 4 \times 10^{-4}$	825.3	825.6 ± 1.2	16.0 ± 0.5	4.58 ± 0.05
	11.3101 $7P_{1/2}$–$5D_{3/2,5/2}$	1.5389		825.6			

This new expression can be applied in the 0.85–16.06 μm wavelength range for o-ray. It gives more accurate refractive indices than other equations given by [13–16] in the 13–16 μm wavelength range. Since the azimuthal angle ϕ is 45° for our $AgGaSe_2$ cutting, we have $d_{eoe} = d_{36} \sin 2\theta_m \cos 2\varphi = 0$ [20], and the wave mixing in type II (oe→e) can not happen. So we can not do the same measurement for the e-ray refractive index of $AgGaSe_2$.

Table 2. The MIR emissions and the corresponding o-ray refractive indices measured in this experiment

IR wavelength predicted from the related transition (μm)	IR wavelength measured in this work (μm)	The o-ray refractive index of $AgGaSe_2$ ($\pm 1 \times 10^{-3}$)
15.9681 $6D_{3/2}$–$7P_{1/2}$	$16.06 \pm 7 \times 10^{-2}$	2.551
16.0836 $6D_{3/2}$–$7P_{3/2}$		
16.0904 $6D_{5/2}$–$7P_{3/2}$		
14.3788 $8S_{1/2}$–$7P_{1/2}$	$14.45 \pm 4 \times 10^{-2}$	2.565
14.4724 $8S_{1/2}$–$7P_{3/2}$		
12.4981 $7P_{3/2}$–$7S_{1/2}$	$12.52 \pm 3 \times 10^{-2}$	2.580
12.5688 $7P_{1/2}$–$7S_{1/2}$		
11.2528 $7P_{3/2}$–$5D_{3/2,5/2}$	$11.28 \pm 2 \times 10^{-2}$	2.587
11.3101 $7P_{1/2}$–$5D_{3/2,5/2}$		

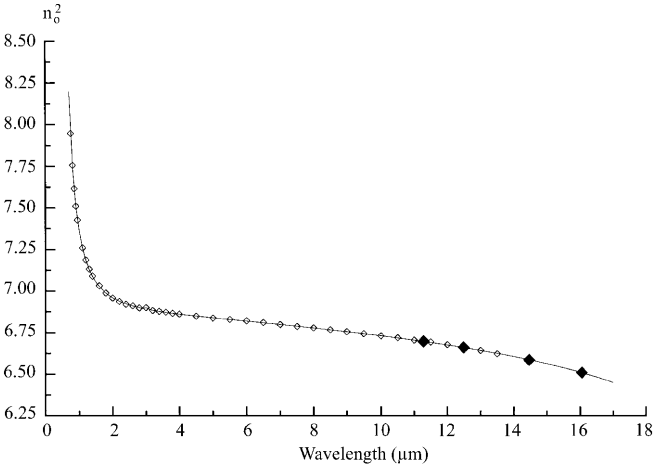

Fig. 7. The refractive-index fitting curve of o-ray for $AgGaSe_2$. The *open diamond points* are the experimental data reported by Boyd et al. (0.85–13.5 μm), and the *solid diamond points* are the experimental data measured in this work (11–16.06 μm)

3 Conclusion

In this paper, we have presented a two-stage up-convertor made of $AgGaSe_2$ and β-BBO crystals. In this two-stage up-convertor, the influence of the walk-off effect in the $AgGaSe_2$ on the up-conversion of the second stage can be

Table 3. The refractive indices of o-ray given by our work and Harasaki et al. for comparison

Wavelength (μm)	The O ray refractive index for $AgGaSe_2$ from this work ($\pm 1 \times 10^{-3}$)	from Harasaki et al. [16]
11.0	2.589	2.589
11.5	2.586	2.586
12.0	2.583	2.583
12.5	2.580	2.580
13.0	2.577	2.577
13.5	2.573	2.573
14.0	2.569	2.570
14.5	2.565	2.567
15.0	2.561	2.563
15.5	2.557	2.559
16.0	2.552	2.555

almost compensated. This up-convertor can up-convert the MIR radiations of the 11–16 μm wavelength range into the 0.8-μm wavelength range where the sensitive PMT can be used for detection. Using this two-stage up-convertor, we measured almost all the ASE spectral lines in the 11–16 μm range at room temperature as the potassium was excited on the 4S–8S and 4S–6D two-photon resonances, except two spectral lines 13.68 μm and 13.70 μm which correspond to the transitions $4F_{5/2,7/2}$–$4D_{5/2}$ and $4F_{5/2,7/2}$–$4D_{3/2}$. Compared with the one-stage up-conversion detection system, the two-stage up-conversion detection system appears to be much more sensitive, has a much better SNR, and is easier to filter against the strong pumping wave.

We also calculated the refractive indices of o-ray for $AgGaSe_2$ from the measurements of the phase-matching angles. Based on our experimental data and Boyd et al.'s data, we extend the Sellmeier equation for the o-ray refractive index to the 16-μm wavelength range. The improved Sellmeier equation can be used in the transmission range of $AgGaSe_2$ from 0.85 μm to 16.06 μm.

Acknowledgements. This project was supported by the National Science Council of the Republic of China under grant No. NSC 88-2112- 09-037.

References

1. P. Canarelli, Z. Benko, A.H. Hielscher, R.F. Curl, F.K. Tittel: IEEE J. Quantum Electron. **QE-28**, 52 (1992)
2. S.Y. Tochitsky, V.O. Petukhov, V.A. Gorobets, V.V. Churakov, V.N. Jakimovich: Appl. Opt. **36**, 1882 (1997)
3. R.S. Feigelson, R.K. Route: J. Cryst. Growth. **104**, 789 (1990)
4. D.A. Russell, R. Ebert: Appl. Opt. **32**, 6638 (1993)
5. B.C. Ziegler, K.L. Schepler: Appl. Opt. **30**, 5077 (1991)
6. R.C. Eckardt, Y.X. Fan, R.L. Byer, R.K. Route, R.S. Feigelson, J. van der Laan: Appl. Phys. Lett. **47**, 786 (1985)
7. R.C. Eckardt, Y.X. Fan, R.L. Byer: Appl. Phys. Lett. **49**, 608 (1986)
8. G.C. Bhar, S. Das, R.K. Route, R.S. Feigelson: Appl. Phys. B **65**, 471 (1997)
9. M.H. Lu, Y.M. Liu: Opt. Commun. **84**, 193 (1991)
10. M.H. Lu, H.W. Wang, H.J. Yeh: Proc. Nat. Sci. Counc. ROC (A) **20**, 288 (1996)
11. E.S. Voronin, V.S. Solomatin, V.V. Shuvalov: Sov. J. Quantum Electron. **8**, 1145 (1978)
12. S.A. Andreev, N.P. Andreeva, I.N. Matveev, S.M. Pshenichnikov: Sov. J. Quantum Electron. **11**, 821 (1981)
13. H. Kidal, J.C. Mikkelsen: Opt. Commun. **9**, 315 (1973)
14. G.C. Bhar: Appl. Opt. **15**, 305 (1976)
15. D.A. Roberts: Appl. Opt. **35**, 4677 (1996)
16. A. Harasaki, K. Kato: Jpn. J. Appl. Phys. **36**, 700 (1997)
17. G.D. Boyd, H.M. Kasper, J.H. Mcfee, F.G. Storz: IEEE J. Quantum Electron. **QE-8**, 900 (1972)
18. F.B. Dunning, Randall G. Hulet: *Atomic, Molecular, and Optical Physics: Atoms and Molecules* (Academic Press, San Diego, California 1996) p. 67
19. R.S. Craxton: IEEE J. Quantum Electron. **QE-17**, 1771 (1981)
20. V.G. Dmitriev, G.G. Gurzadyan, D.N. Nikogosyan: *Handbook of Nonlinear Optical Crystal* (Springer, Berlin, Heidelberg 1991) p. 84
21. D.A. Kleinman, G.D. Boyd: J. Appl. Phys. **40**, 546 (1969)